Performance analysis for indoor wireless systems employing directional antennas

A H. Wong* Michael Neve†

Kevin Sowerby‡

*University of Auckland,

†University of Auckland, mj.neve@auckland.ac.nz

‡University of Auckland, kw.sowerby@auckland.ac.nz

Performance analysis for indoor wireless systems employing directional antennas

A.H. Wong, M.J. Neve and K.W. Sowerby

Abstract: Using indoor propagation measurements, an investigation of the influence of antenna directivity on the performance of an indoor wireless system is presented. By comparing the path loss data measured from collocated omnidirectional and directional antennas (at different orientations), it is shown that the 'effective' directivity of a directional antenna is heavily dependent on the surrounding environment. Antenna directivity and orientation are shown to influence the level of interference within a system and, therefore, affect overall system performance. Analysis of a simple indoor system with two cochannel base stations showed that the use of directional antennas could either enhance or degrade system performance, relative to a system using omnidirectional antennas. In the best case the use of directional antennas decreased outage probability by 56%, while in the worst case the outage probability increased by 66%.

1 Introduction

Indoor wireless systems are attracting much interest due to the commercial success of the IEEE 802.11*x* and Bluetooth technologies. These systems, especially the derivatives of the IEEE 802.11 standard, can provide broadband access to a high density of users. However, this high user density means that these systems are particularly vulnerable to cochannel interference. Fortunately this interference can (to some degree) be minimised with careful system planning. The placement of indoor [1] and outdoor [2] base stations has been shown to have significant impact on system interference levels and, hence, on the performance of indoor wireless systems. For simplicity, this research has usually assumed the use of omnidirectional antennas. However, the selection and deployment of directional antennas can also influence the interference-limited performance of a system. Accordingly, this paper discusses the impact of the selection and orientation of antennas on overall performance of an indoor wireless system.

2 Indoor deployment and antenna selection

In contrast to the deployment of outdoor cellular systems, in which a few base stations are used to provide service to a relatively large area, the deployment of indoor wireless systems often involves a relatively large number of base stations, each serving a small area. This difference in the deployment strategy can affect the selection of antennas for the base stations. In indoor systems, aesthetics and cost are two particularly important factors. Since indoor base stations are often installed at the users' premises, the antennas employed should be compact, inexpensive and preferably hidden from the view of the users.

2.1 Antenna selection options

The candidates for base station antennas can be divided into two categories: 'smart' and 'dumb' antennas. The class of smart antennas refers to antenna systems with a degree of 'intelligence' that enables the continual adaptation of their radiation characteristics to best cope with changing conditions. These smart (or MIMO, multiple-input multiple-output) antenna systems use multiple antenna elements to exploit diversity of propagation paths between transmitters and receivers, which can significantly increase system capacity over traditional (dumb) antenna systems [3]. MIMO systems are an attractive technical solution for indoor environments where high capacity and user density are needed. However, their commercial realisation is being impeded by their inherently high RF (radiofrequency) and baseband signal processing hardware costs [4].

In comparison, dumb antennas have fixed radiation characteristics. Once manufactured and installed in desired locations, there is no easy way to modify their characteristics except by reorientation. The implementation costs of these antennas are relatively low since only a single RF frontend is needed for each antenna and no complex signal processing hardware is needed. These antennas can be categorised as either omnidirectional or directional. Omnidirectional antennas (such as dipoles and monopoles) transmit energy evenly in all directions in the azimuthal plane, whereas directional antennas (such as microstrip patches and fixed arrays) focus energy in a particular direction. Microstrip patches, in particular, are attractive candidates for indoor deployment because of their low profile and low cost.

2.2 Orientation selection

A new degree of freedom is introduced in the deployment of indoor wireless systems when fixed-radiation pattern directional antennas are employed instead of omnidirectional antennas. A commonly held belief is that directional antennas can be used to 'contain' signals within a specified area due to their directivity. However, there are neither

IEE Proceedings online no. 20059011

doi:10.1049/ip-com:20059011

Paper first received 19th December 2003 and in revised form 8th September 2004

The authors are with the Department of Electrical and Computer Engineering, The University of Auckland, Private Bag 92019, Auckland, New Zealand

E-mail: kw.sowerby@auckland.ac.nz

guidelines to the orientation of directional antennas for optimal performance nor measures for quantifying the improvement that directional antennas might afford system performance. It is very difficult to estimate this effect in an indoor environment suffering multipath propagation. Also, the antennas are likely to be in close proximity to building structures, which can modify the radiation characteristics of the antennas. Therefore, field measurement of directional antennas is necessary to allow the evaluation of their impact on overall system performance.

3 Propagation study

A propagation measurement campaign was conducted in the School of Engineering Building at The University of Auckland [5]. The measurement environment was a typical multistorey, reinforced concrete structure with a floor area of 18.5 m × 18.5 m. Measurements were performed on the eighth floor of the building, which contains a concrete central services core surrounded by many fixed-partitioned rooms, as shown in Fig. 1.

Two transmitting stations, which transmitted at slightly different frequencies about 1880 MHz, were located in opposing diagonal corners of the corridors in the floor area. Individual measurements from both transmitters were performed at 42 receiver locations, which are shown by the '×' symbols in Fig. 1. Measurements were repeated for different antenna configurations at the two transmitters.

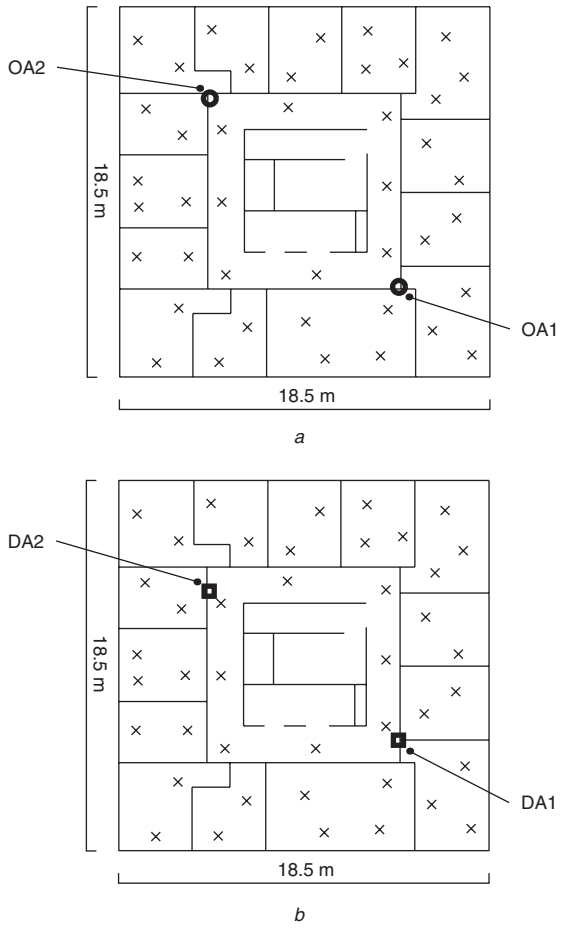

Fig. 1 *Floor plan of the measurement environment*
'×' represents receiver locations; 'o' and '□' denote an omnidirectional and a directional antenna, respectively. The omnidirectional and directional antennas are essentially collocated
a Locations of omnidirectional antennas
b Locations of directional antennas

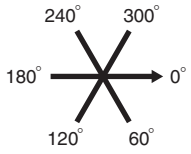

Fig. 2 *Orientations of a directional antenna considered*

Seven different antenna configurations were used at each transmitter; namely an omnidirectional discone antenna (labelled OA1 and OA2) and a patch antenna (labelled DA1 and DA2) pointing to one of six orientations in the azimuthal plane. Figure 2 shows the orientations of the patch antennas labelled from 0° to 300° clockwise (in 60° steps).

The transmitter system used in the propagation measurements represented a transmitting base station that was fitted with either an omnidirectional discone or a directional patch antenna. The discone antenna provided a performance reference level in subsequent analysis. The patch antenna had a 3 dB beamwidth of 65° and a gain of 5.8 dB relative to the discone antenna. An antenna rotator was used to obtain accurate and repeatable orientations of the patch antenna. Continuous-wave (CW) transmissions were used at a carrier frequency of 1880 MHz. The receiver system represented a mobile user moving around the measurement environment. It consisted of a folded dipole antenna mounted on a rotating arm of 0.5 m in radius, together with an automated antenna rotator, a test receiver and a computer with appropriate control software. A total of 360 evenly spaced measurements of the instantaneous received signal power (in dBm) were recorded in one revolution of the rotating arm. From the measured data, an estimate of the local mean path loss PL and Rician fading statistics were obtained at each measurement location. Rician K-factors were estimated using the method-of-moments [6].

The measurement campaign produced a high-resolution propagation database of narrowband path losses for the given indoor environment. Measurements of the local mean path losses were performed at a large number of potential user locations for a number of antenna orientations. The effects of short-term fading were removed by averaging the data measured along a small circular locus about the desired location. An advantage in using this measurement database was the elimination of the need for an accurate propagation model in analysing wireless system performance.

Contour maps of path losses were generated for a single transmitter under three antenna configurations: (*a*) discone antenna OA1, (*b*) patch antenna DA1 at 120°, and (*c*) DA1 at 300°, as shown in Fig. 3. The light-shaded regions on the contour map represent low path losses, whereas the dark-shaded regions correspond to high path losses. The smooth contour lines were generated by interpolation based on measured data and no propagation model has been used. The interpolation process can be inaccurate through walls and obstacles that cause a sudden change in path losses. Therefore, the central core area of the floor plan was deliberately masked because measurements from that area were not used. The contour maps do, however, illustrate the general coverage patterns of different antenna configurations. In Fig. 3*a*, which shows the contour map for a transmitter with an omnidirectional antenna, a deep shadow (dark region) can be seen at the upper-left corner of the floor plan, diagonally opposing the transmitter at the lower-right corner. This is an anticipated result and is due to the steel-reinforced concrete core which causes high signal

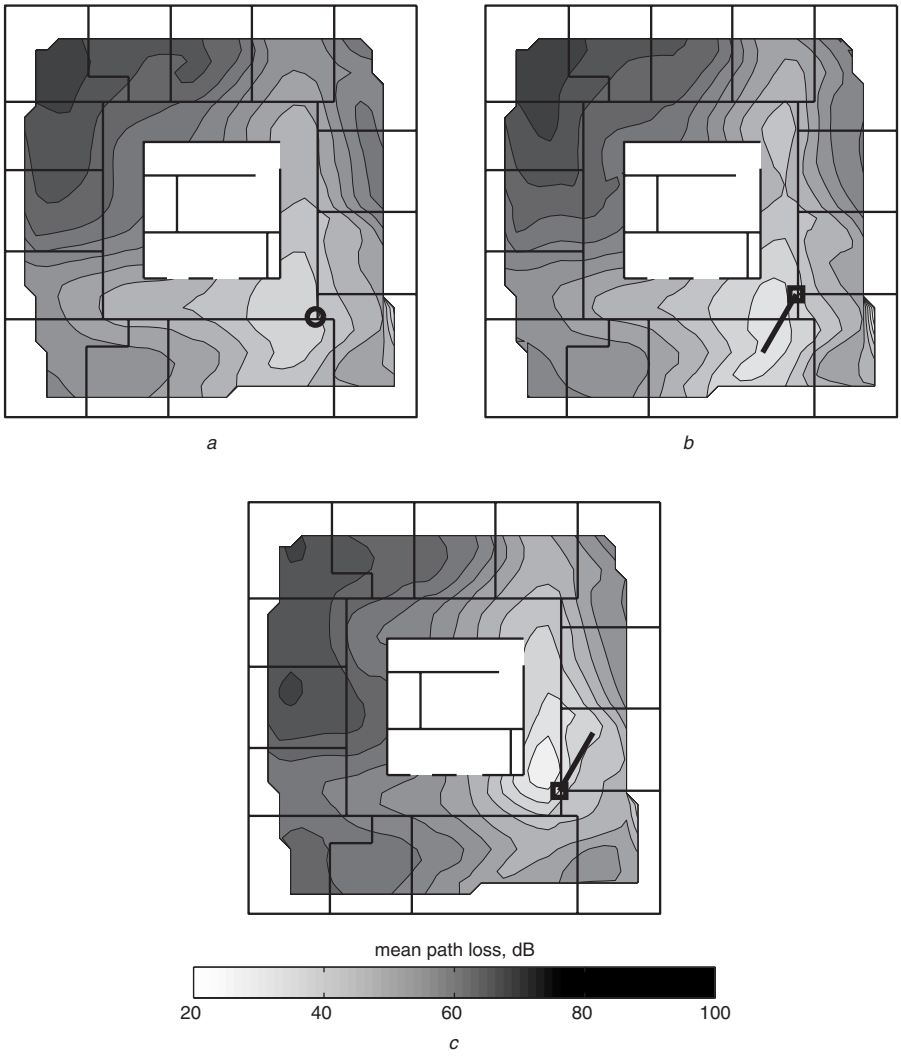

Fig. 3 *Mean path loss contour maps for antennas*
Note that the contour lines are 6 dB apart
a OA1
b DA1 at 120°
c DA1 at 300°

attenuation. A channelling effect is observed in the corridors having a line-of-sight orientation with the transmitter. The overall shape of the contour map is symmetrical along the diagonal axis of the floor plan. This is also expected due to the symmetrical radiation pattern of the omnidirectional antenna in the azimuthal/horizontal plane.

The effect of the surrounding environment upon the effective radiation characteristics of a directional antenna is illustrated in Fig. 3*b*, which shows the contour map of path losses for a collocated transmitter with directional antenna DA1 at 120°. The contour map for this antenna configuration is very similar to that of the omnidirectional antenna. All the major features from that of the omnidirectional antenna, such the dark shadow at the upper-left corner, the channelling effect and the line of symmetry, can also be found in this contour map. The directive property of the antenna at this orientation appears to be significantly impeded; probably as a result of the coupling with nearby building structure and objects. In contrast, Fig. 3*c* shows the contour map of path losses for the same transmitter with antenna DA1 but with an orientation of 300°. A deep shadow can still be seen in the upper-left corner of the floor plan. This shadow, however, extends towards the lower-left side of the plan. Channelling of the signal in the corridors is still observed, but it becomes asymmetrical with a stronger effect in the direction of the antenna. This shows that the effective directive property of a directional antenna can be dependent on its orientation relative to the environment. These results suggest that in the design of indoor wireless systems, it is necessary to study the implications of effective antenna directive property upon system performance.

4 Downlink system performance

Using the measured data from the measurement campaign outlined in Section 3, a system model has been developed to evaluate the influence of antenna orientation on indoor downlink system performance. A two-cochannel base station deployment scenario was considered. Each base station was configured with either an omnidirectional antenna or a directional antenna at a particular orientation. Thus, there were seven possible antenna configurations on each base station, and a total of 49 combinations in the two-base-station system. A user connected to one base station could receive cochannel interference from the other base station. Two connection scenarios to the base stations were considered: static and dynamic connections. In the static connection scenario, users were assigned to a fixed base

station and they stayed connected to that base station regardless of their location and the received signal strength. This represents the scenario in which no handoff between base stations is possible. Alternatively, under the dynamic connection scenario, users connected to the base station with stronger average received signal strength at their respective locations. This represents the situation in which handoff between base stations can occur. The received signal of the user was assumed to experience either Rayleigh or Rician fading.

A system model adopted from [1], which employs the DS-CDMA multiple-access scheme with BPSK modulation, was assumed for system performance analysis. It was further assumed that there were K simultaneous users connected to each of the base stations. System performance was quantified by the average outage probability over all possible user locations across the entire floor area. Outage probability is defined as the probability that the bit-error-rate (BER) exceeds a specific threshold. The BER of the downlink transmission can be approximated by [1]

$$BER \approx \Phi\left[\frac{1}{\sqrt{\frac{\alpha}{3N}(K-1+\beta)}}\right] \quad (1)$$

where $\Phi(\cdot)$ is the complementary Gauss probability integral, α is the voice activity factor (assumed to be 0.5), N is the processing gain (assumed to be 511) and K is the number of users in each cell. The variable β is location dependent, and is given by

$$\beta = \frac{KP_{\text{int}}}{P_{\text{des}}} \quad (2)$$

where P_{int} and P_{des} are the received power from the interfering and desired base station, respectively. While [1] assumes Rayleigh fading on all desired and interfering signals, in this paper Rician fading of the received signals is also considered. A Rician model allows for a dominant signal component in addition to other multipath (Rayleigh) components [7, pp. 139–140]. For indoor environments where a direct line-of-sight (LOS) path is likely to exist between a user and its desired base station, a Rician fading model is more appropriate than a Rayleigh fading model.

Since N, K and α were all fixed as system parameters, the BER can be fully characterised by the value of β. Using this expression for the BER, the average outage probability for the given system can then be estimated via simulation [1] or solved analytically. Simulation and analytical results are presented in Sections 4.1 and 4.2, respectively.

Both simulation and analytic techniques are equally applicable to both omnidirectional and directional antennas. However the use of omnidirectional antennas is assumed in the development of the techniques in accordance with previous research [1, 2]. The effects of directional antennas are considered in Section 4.3.

4.1 Monte Carlo simulation

Monte Carlo simulation was used to model the short-term fading of the received signal. In each iteration of the simulation, a user location was selected randomly from all possible locations in Fig. 1, and the instantaneous BER of the downlink transmission was determined by substituting P_{int} and P_{des} in (1) and (2) with Rician random variables (which were squared to obtain power units). A Rician random variable was generated by combining a complex Rayleigh random variable with a constant that represented the dominant signal component. The relative amplitudes of the Rayleigh random variable and the constant were

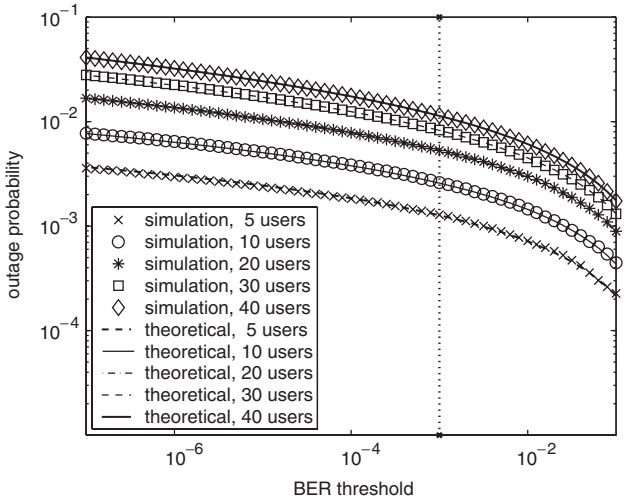

Fig. 4 *Comparison of the average outage probability determined by simulation and analytical solution for the dynamic scenario with Rician fading between antennas OA1 and OA2*
BER threshold used in the analysis is shown by a dotted line at the value of 10^{-3}

determined by the statistics collected in the field measurements as described in Section 3. The instantaneous BER was compared with the specified BER threshold to determine whether an outage had occurred. The average outage probability for the entire floor area was estimated by averaging these outage probabilities over 10^6 iterations. The number of iterations was determined experimentally to give repeatable results. The simulation was repeated for each of the 49 combinations of antenna configurations.

Using the measured data for the configuration in which both antennas are omnidirectional (OA1 and OA2), the average outage probability was determined as a function of BER threshold for various numbers of users K and is shown in Fig. 4. At any BER threshold, the outage probability increases as the number of users increases (and there is increased interference in the system).

4.2 Analytical solution

The average outage probability of a general mobile radio system can also be determined analytically. For the case of a Rician desired signal and a single Rician interferer, the outage probability is given by [8]

$$P_{\text{out}} = \boldsymbol{Q}\left[\sqrt{\frac{2K_{\text{I}}R_{\text{I}}}{b_1+R_{\text{I}}}}, \sqrt{\frac{2K_0 b_1}{b_1+R_{\text{I}}}}\right] - \frac{b_1}{b_1+R_{\text{I}}}\exp\left[-\frac{K_{\text{I}}R_{\text{I}}+K_0 b_1}{b_1+R_{\text{I}}}\right] I_0\left(\frac{\sqrt{4K_{\text{I}}K_0R_{\text{I}}b_1}}{b_1+R_{\text{I}}}\right) \quad (3)$$

where $\boldsymbol{Q}(\cdot)$ is the Marcum Q-function, $I_0(\cdot)$ is the modified Bessel function of the first kind of zero order, K_0 and K_{I} are the K-factors of the desired and interfering signals, respectively, R_{I} is the protection ratio and $b_1 = \sigma_0^2/\sigma_{\text{I}}^2$, where σ_0^2 and σ_{I}^2 are the variances of the multipath components of the desired and interfering signals, respectively. When both K_0 and K_{I} tend to zero, so that neither received signal has a dominant multipath component, (3) reduces to give the outage probability for Rayleigh faded signals.

In the calculation of the local outage probability, the variables K_0, K_{I} and b_1 were determined by field

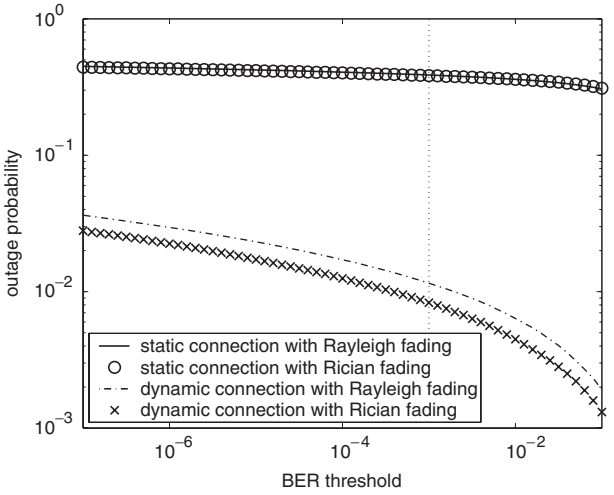

Fig. 5 *Analytically determined average outage probability for both static and dynamic scenario with Rayleigh and Rician fading between antennas OA1 and OA2*
Number of users $K = 30$, BER threshold used in the analysis is shown by a dotted line at the value of 10^{-3}

measurements at the individual user locations outlined in Section 3. The protection ratio R_I is the reciprocal of $\beta(R_I = 1/\beta)$ that achieves the specified BER in (1). The average outage probability for the system was then determined by averaging the local outage probabilities at all possible user locations across the floor area.

In Fig. 4, the analytically determined average outage probability for the same system from Section 4.1 is overlaid on the simulation results. The strong similarity of the results implies that both techniques provide good estimates of the outage probability for the given system. Using the same set of measured data, the average outage probability was determined analytically as a function of BER threshold for various fading and connection scenarios, as shown in Fig. 5. It can be seen that there is a significant reduction in outage probability under the dynamic connection scenario compared with that of the static connection scenario. At a BER threshold of 10^{-3}, the outage probability for the static connection scenario with Rician fading is nearly 50 times greater than that of the dynamic connection scenario with Rician fading.

In the comparison between Rayleigh and Rician fading, it is observed that the outage probabilities follow the same trend under both fading scenarios as a function of BER threshold. Although no significant difference is observed between the outage probabilities between Rayleigh and Rician fading for the static connection scenario, it is evident that the outage probabilities of the Rician fading case are lower than those of the Rayleigh fading case under the dynamic connection scenario. A 30% (1.5 dB) drop in the outage probability is observed at a BER of 10^{-3}. This result can be explained by the lower variability of Rician fading due to the presence of a dominant signal component.

4.3 Implications of antenna directivity on system performance

The influence of antenna directivity on indoor downlink system performance has been evaluated under the dynamic connection scenario with Rician fading. The average outage probability of the system with various antenna configurations has been determined analytically as outlined in Section 4.2. A BER threshold of 10^{-3} was used in the analysis, as typically required for voice [9]. The configuration between two omnidirectional antennas (OA1 and OA2) was considered as the reference scenario and the basis of comparison. The average outage probabilities of other configurations were normalised to that of the reference scenario and are summarised in Table 1. A normalised value less than unity implies that the average outage probability of the system is lower than the reference (omnidirectional) scenario. In contrast, a normalised value greater than unity implies that the corresponding antenna configuration has a relatively high average outage probability and, therefore, inferior performance. The normalised values are in the range 0.44–1.66 in Table 1, which indicate that a 56% reduction to a 66% increase in system performance resulted solely from changing the orientations of the directional antennas. Figure 6 shows the minimum and maximum normalised outage probabilities for various BER threshold values. Note that the normalised values are virtually invariant with the BER threshold. This suggests that the impact of antenna orientations on system performance is independent of the BER threshold, at least over the range of BERs considered in this study.

Figure 7 shows the antenna configurations for the reference case (omnidirectional antennas), the lowest and highest average outage probabilities. The average signal-to-interference ratio (SIR) is shown in contour maps overlaid on the floor plans. The light-shaded regions represent a high SIR, whereas the dark-shaded regions correspond to a low SIR. When the average power level of the interfering signal is close to that of the desired signal (a low SIR), the chance of an outage occurrence increases. The change in the orientations of the directional antennas effectively changes the distribution of the high and low SIR regions. In Fig. 7*b*, there is a higher fraction of high SIR (light-shaded) regions than in Fig. 7*a*. This implies a higher overall SIR, and therefore a lower average outage probability, in Fig. 7*b* compared to Fig. 7*a*. It is noted that the antennas are

Table 1: Normalised outage probabilities for different antenna configurations

		Antenna	Antenna DA1					
		OA1	0°	60°	120°	180°	240°	300°
Antenna OA2		1.00	1.10	0.90	1.28	1.30	0.92	0.68
	0°	0.87	1.36	1.01	1.06	1.00	0.92	0.63
	60°	1.45	0.88	0.70	1.05	1.66	1.05	0.48
Antenna DA2	120°	1.00	0.44	0.44	0.77	0.95	0.93	0.48
	180°	0.77	0.87	0.93	0.95	0.88	0.86	0.58
	240°	1.15	0.83	1.21	1.31	1.15	1.13	0.69
	300°	1.04	1.03	1.09	1.18	1.05	0.99	0.53

pointing away from each other in the configuration in Fig. 7*b*. This minimises the self-interference in the system. However, this configuration might increase the external interference to (and from) nearby systems since more power is directed outward from the building. In contrast, the antennas are facing each other in the configuration of highest average outage probability in Fig. 7*c*. This configuration would minimise external interference at the expense of increased self-interference. Thus, by careful selection of the orientations of directional antennas, system planners can control the relative levels of self-interference and external interference in an indoor environment and, therefore, co-ordinate the performance of self and adjacent wireless systems.

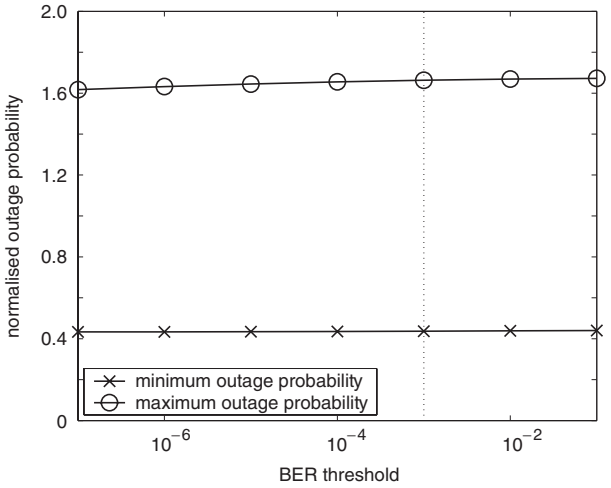

Fig. 6 *Analytically determined minimum and maximum normalised outage probabilities as a function of BER threshold for the dynamic scenario with Rician fading*

By close examination of Table 1, it is noted that the highest outage probability configuration corresponds to the combination of directional antennas DA1 at 180° and DA2 at 60°. When considering the two directional antennas in isolation, namely the configurations between directional antenna DA1 and omnidirectional antenna OA2, the highest outage probability configuration was observed at the same orientation of 180° for DA1. Similarly, directional antenna DA2 at 60° gave the highest outage probability from the configurations between antennas OA1 and DA2. This allows us to determine the highest outage probability configuration for two directional antennas with fewer measurements, namely two sets of

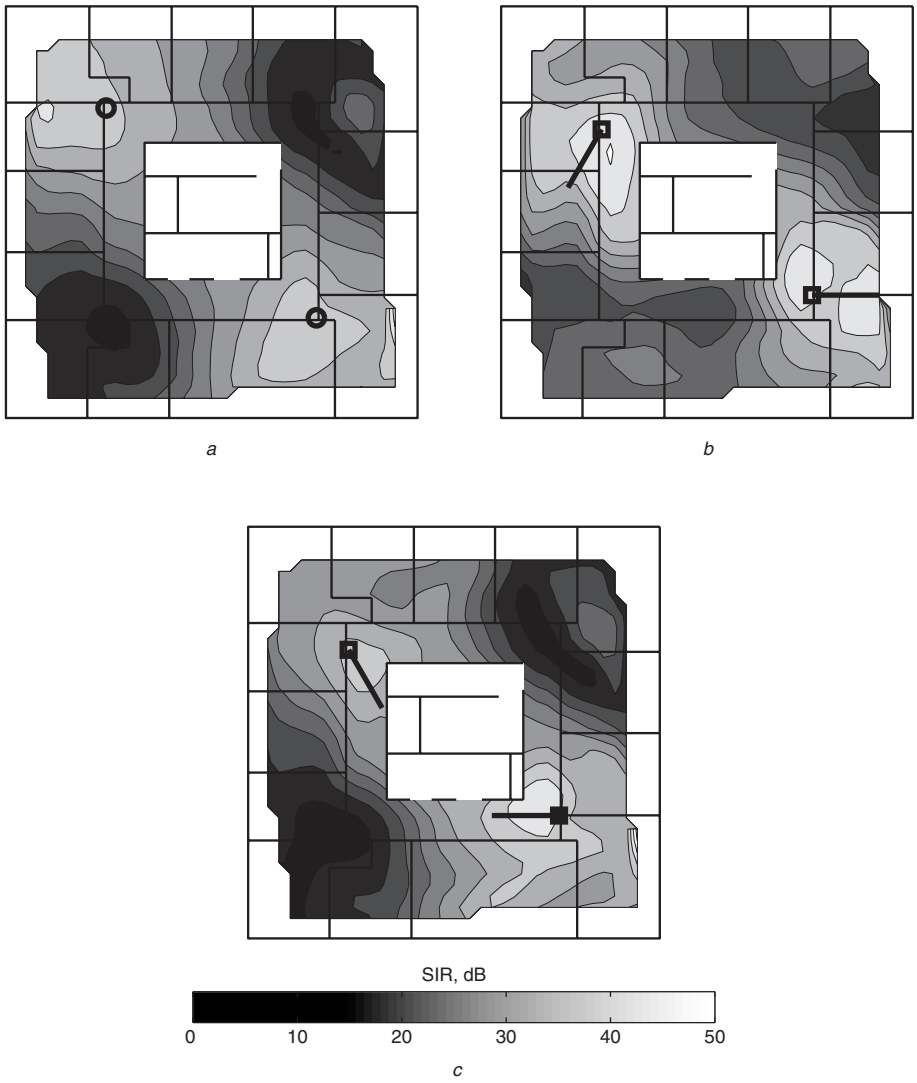

Fig. 7 *SIR contour maps*
Note that the contour lines are 6 dB apart
a Reference (omnidirectional) scenario ($P_{out} = 1$)
b Antenna configuration with the lowest average outage probability ($P_{out} = 0.44$)
c Antenna configuration with the highest average outage probability ($P_{out} = 1.66$)

measurements between a directional and an omnidirectional antenna.

This method of prediction, however, was not as accurate for the determination of the antenna configuration for the lowest outage probability. From the configurations between directional antenna DA1 and omnidirectional antenna OA2, the lowest outage probability was observed at the orientation of 300° for DA1. Similarly, the lowest outage probability was observed at an orientation of 180° for DA2 for configurations between antennas OA1 and DA2. At these orientations of their respectively directional antennas, a normalised outage probability of 0.58 was resulted, which is close to, but higher than, the minimum outage value of 0.44. The difference between the prediction and actual measurement highlights the complexity of the interaction between the two antennas and the environment.

5 Conclusions

Measured data from a propagation study in an indoor environment shows that the effective directivity of directional antennas is heavily dependent upon the surrounding environment. The effect of antenna directivity upon system performance was evaluated for an indoor wireless system consisting of two cochannel base stations. Rician fading was assumed. System performance was quantified in terms of average outage probability. With reference to the system using omnidirectional antennas, both significant reductions and increases in average outage probability were observed in the same systems that employ different orientations of directional antennas. In the best case, the use of directional antennas decreased outage probability by 56%, while in the worst case the outage probability increased by 66%. While a decrease in average outage probability represents increased system performance, an increase in average outage probability might be tolerated if it was the cost of reducing interference to nearby wireless systems by directing antennas inwards.

6 References

1 Butterworth, K.S., Sowerby, K.W., and Williamson, A.G.: 'Base station placement for in-building mobile communication systems to yield high capacity and efficiency', *IEEE Trans. Commun.*, 2000, **48**, (4), pp. 658–669

2 Pais, A.V., Sowerby, K.W., and Neve, M.J.: 'Outdoor-to-indoor signal correlation and its influence on indoor system performance at 2 GHz', *Electron. Lett.*, 2003, **39**, (2), pp. 236–238

3 Foschini, G.J., and Gans, M.J.: 'On limits of wireless communications in a fading environment when using multiple antennas', *Wirel. Pers. Commun.*, 1998, **6**, (3), pp. 311–335

4 Agee, B.G.: 'Efficient allocation of RF transceiver resources in spatially adaptable communication networks'. Proc. Workshop on Advances in Smart Antennas for Software Radios, Proc. 13th Virginia Tech/MPRG Symp. on Wireless Personal Communications, Blacksburg, VA, USA, 4–6 June 2003, pp. 60–76

5 Wong, A.H., Neve, M.J., and Sowerby, K.W.: 'Performance analysis for indoor wireless systems employing directional antennas using a Rician fading model'. Proc. 13th Virginia Tech/MPRG Symp. on Wireless Personal Communications, Blacksburg, VA, USA, 4–6 June 2003, pp. 9–18

6 Greenstein, L.J., Michelson, D.G., and Erceg, V.: 'Moment-method estimation of the Ricean *K*-factor', *IEEE Commun. Lett.*, 1999, **3**, (6), pp. 175–176

7 Parsons, J.D.: 'The mobile radio propagation channel' (Wiley, Chichester, New York, 2000, 2nd edn.)

8 Tjhung, T.T., Chai, C.C., and Dong, X.: 'Outage probability for a Rician signal in *L* Rician interferers', *Electron. Lett.*, 1995, **31**, (7), pp. 532–533

9 Chockalingam, A., Dietrich, P., Milstein, L., and Rao, R.: 'Performance of closed-loop power control in DS-CDMA cellular systems', *IEEE Trans. Veh. Technol.*, 1998, **47**, (3), pp. 774–789